

Non-holonomic Quantum Devices

V. M. Akulin,¹ V. Gershkovich,² and G. Harel³

¹*Laboratoire Aimé Cotton, CNRS II, Bâtiment 505, 91405 Orsay Cedex, France*

²*Institut des Hautes Etudes Scientifiques, Bures-sur-Yvette, France*

³*Department of Physics and Astronomy, Vrije Universiteit, De Boelelaan 1081, 1081 HV Amsterdam, The Netherlands*
(December 19, 2000)

We analyze the possibility and efficiency of non-holonomic control over quantum devices with exponentially large number of Hilbert space dimensions. We show that completely controllable devices of this type can be assembled from elementary units of arbitrary physical nature, and can be employed efficiently for universal quantum computations and simulation of quantum field dynamics. As an example we describe a toy device that can perform Toffoli-gate transformations and discrete Fourier transform on 9 qubits.

PACS numbers: 03.67.-a, 03.65.-w, 32.80.Qk

I. INTRODUCTION

What is the difference between a classical and a quantum device? Clearly it is not in the physical laws governing their dynamics, since Classical Mechanics follows from Quantum Mechanics as a limiting case, when mechanical action for each degree of freedom is much larger than the Planck constant \hbar . Hence, all classical devices are quantum as well, and the basic difference between them is rather in the quantities of interest and in the interactions under control. Typically, the operators of main physical quantities have smooth dependence of their semiclassical matrix elements on the indices numerating the energy eigenstates, and therefore a state of the device is characterized by the position of the center of the Ehrenfest wave packet in phase space. The average quantities are determined as functions of this position, whereas the finite packet width results in uncontrolled “quantum noise” and is considered as an obstacle for the correct operation of the classical device in the quantum limit.

The situation is different in the essentially quantum limit, where the action for each degree of freedom is of the order of \hbar . Then, the matrix elements are not smooth anymore, and the consistent description of an N -level device relies not only on quantum averages of operators, but also on all their higher moments as well. Such description requires exhaustive information about the state of the system, as given by a vector in the N -dimensional Hilbert space of the system. Building a completely controlled quantum device in practice implies control over all the moments and therefore is a challenging task. It promises, however, adequately important practical benefits: coherent control of molecules, quantum cryptography, and quantum computation are some of the potential applications [1–15].

In this paper we describe a scheme for constructing completely controllable quantum devices. We show that quantum systems perturbed in a certain time-dependent way become “non-holonomic”, which means that as a result of the perturbation all global constraints on the

dynamics are removed and the system becomes fully controlled (Sec. II). We then describe a simple, completely controllable “unit cell” that can serve as a building block for compound devices of arbitrary size (Sec. III), and show in particular that it can implement the Toffoli gate (Appendix A). We give examples of compound devices that can be employed efficiently for universal quantum computations and simulation of quantum field dynamics (Sec. IV). Finally, we describe a toy device that can perform quantum computations on 9 qubits and show in particular how it can perform the discrete Fourier transform on 9 qubits (Sec. V).

II. NON-HOLONOMIC CONTROL

The idea of controlling a system by forcing it to have globally unconstrained—non-holonomic—dynamics is natural, since in order to ensure an arbitrary evolution one has first to get rid of the restrictions posed by the existing integrals of motion and all other constraints. In the non-holonomic control scheme, the system evolution is determined by an unperturbed Hamiltonian \hat{H}_0 and a number of perturbations $C_i \hat{P}_i$ of fixed operator structure \hat{P}_i and controllable strengths C_i that are applied to the system, so that the evolution is given by the time-dependent Hamiltonian

$$\hat{H}(t) = \hat{H}_0 + \sum_i C_i(t) \hat{P}_i. \quad (1)$$

The system becomes non-holonomic and completely controllable if the commutators of all orders of \hat{H}_0 and the \hat{P}_i span the space of Hermitian operators in the Hilbert space of the system, that is, if an arbitrary Hermitian operator can be represented as a linear combination of the operators

$$\hat{H}_0, \hat{P}_i, [\hat{H}_0, \hat{P}_i], [\hat{P}_i, \hat{P}_j], \dots, [\hat{P}_i, [\hat{P}_j, \hat{P}_k]], \dots \quad (2)$$

Note that at most N^2 linearly independent terms are needed for an N dimensional Hilbert space.

The control scheme consists of two steps: (i) verification that the perturbations induce non-holonomic dynamics; and (ii) finding particular time dependencies for the perturbations that effect a given desired control. Step (i) is straightforward—by inspecting the commutation relations between the explicitly written Hamiltonian and perturbation operators, one checks if the system under consideration is indeed non-holonomic. But step (ii) requires more art—one has to put the system in such conditions that all unwanted outcomes, present in abundance in a system with no constraints, experience a destructive quantum interference.

Let us consider a quantum system of $N = 2^n$ levels, composed of n interacting two-level subsystems. To be specific we speak about two-level atoms in a laser field, although it could as well be any other quantum object, such as interacting spins in a magnetic field, Josephson junctions, Rydberg atoms, rotating molecules, quantum dots on a surface, etc. The only requirement is that the object must be subjected to a non-holonomic control, since only in this case it can perform any desired operation, no matter what the physical interactions in the system are. The choice of a practical realization of a non-holonomic system will therefore depend mainly on optimization of technical parameters such as simplicity and cost-effectiveness of construction, lifetime of quantum coherence [16], precision of available controls, and so on.

A crucial issue that determines the strategy of construction is the required extent of immediate universality of the control. In principle, one can think about complete and direct physical control over a 2^n -level quantum system, even for a large n , which implies the ability to ensure an arbitrary evolution of the system, given by any predetermined $2^n \times 2^n$ unitary matrix \hat{U} , and which requires 4^n physical control parameters. For this purpose one should find an algorithm that determines these controls for any given \hat{U} . It might be difficult to find such algorithm, and even if found, its application will require an enormous computational work that grows exponentially with n , and will therefore be intractable. In addition, the cost of physically implementing the huge number of 4^n control parameters seems too high a price to pay for this kind of universality, which may not even be needed for practical purposes. For these reasons, one should presumably give up direct universality and search for specialized ways to build quantum devices for each particular task, with number of controls that is not exponentially larger than what is specifically needed.

III. COMPLETELY CONTROLLED UNIT CELL

One way to construct a completely controlled but not immediately universal quantum device is to build it up from small parts, “unit cells”, each of which is non-holonomic and therefore directly and universally controllable. The proper functioning of the device relies then on the appropriate connection of the cells [17]. In this way

the universality of the device is obtained indirectly, not by applying a huge number of controls, but by smartly connecting the cells and choosing the sequence of operations performed. There is no general prescription how to construct a particular device; this requires expertise in the art of “programming” the operations of the cells and their interactions.

A. Cell structure

An example of a completely controlled unit cell is shown in Fig. 1. It consists of three two-level atoms, each with ground and excited states $|0\rangle$ and $|1\rangle$, having distinct transition frequencies ω_1^a , ω_2^a , and ω_3^a . The atoms have dipole-dipole interaction between themselves and are coupled to two external fields: an electromagnetic field $E_\omega = \mathcal{E}_\omega \cos \omega t$ of nearly resonant frequency ω , and a static electric field E_S . The dipole-dipole interaction is fixed and determines the principal, unperturbed Hamiltonian of the system, \hat{H}_0 , while the external fields provide two controllable perturbations, \hat{P}_ω and \hat{P}_S . The Hilbert space of the system has a “computational basis” of $N = 2^3 = 8$ states, $|x\rangle \equiv |x_2 x_1 x_0\rangle \equiv |x_2\rangle |x_1\rangle |x_0\rangle$, $x = 0, 1, \dots, 7$, where the state of the i th atom encodes the i th binary digit of $x = \sum_{r=0}^2 x_r 2^r$ as a qubit [see Fig. 1(b)]. The crucial requirement is the non-holonomic character of the interaction. It implies that \hat{H}_0 , \hat{P}_ω , \hat{P}_S , and their commutators of all orders span the linear space of 8×8 Hermitian matrices [18]. This is indeed the case for the system shown in Fig. 1, which has principal Hamiltonian and perturbations given, in the computational basis and assuming resonant approximation, by the matrices

$$\hat{H}_0 = \begin{pmatrix} 0 & 0 & 0 & 0 & 0 & 0 & 0 & 0 \\ 0 & A_1 & D_{12} & 0 & D_{13} & 0 & 0 & 0 \\ 0 & D_{21} & A_2 & 0 & D_{23} & 0 & 0 & 0 \\ 0 & 0 & 0 & A_{12} & 0 & D_{23} & D_{13} & 0 \\ 0 & D_{31} & D_{32} & 0 & A_3 & 0 & 0 & 0 \\ 0 & 0 & 0 & D_{32} & 0 & A_{13} & D_{12} & 0 \\ 0 & 0 & 0 & D_{31} & 0 & D_{21} & A_{23} & 0 \\ 0 & 0 & 0 & 0 & 0 & 0 & 0 & A_\sigma \end{pmatrix}, \quad (3)$$

$$C_\omega \hat{P}_\omega = \begin{pmatrix} 0 & V_1 & V_2 & 0 & V_3 & 0 & 0 & 0 \\ V_1 & 0 & 0 & V_2 & 0 & V_3 & 0 & 0 \\ V_2 & 0 & 0 & V_1 & 0 & 0 & V_3 & 0 \\ 0 & V_2 & V_1 & 0 & 0 & 0 & 0 & V_3 \\ V_3 & 0 & 0 & 0 & 0 & V_1 & V_2 & 0 \\ 0 & V_3 & 0 & 0 & V_1 & 0 & 0 & V_2 \\ 0 & 0 & V_3 & 0 & V_2 & 0 & 0 & V_1 \\ 0 & 0 & 0 & V_3 & 0 & V_2 & V_1 & 0 \end{pmatrix}, \quad (4)$$

$$C_S \hat{P}_S = \begin{pmatrix} 0 & 0 & 0 & 0 & 0 & 0 & 0 & 0 \\ 0 & \Delta_1 & 0 & 0 & 0 & 0 & 0 & 0 \\ 0 & 0 & \Delta_2 & 0 & 0 & 0 & 0 & 0 \\ 0 & 0 & 0 & \Delta_{12} & 0 & 0 & 0 & 0 \\ 0 & 0 & 0 & 0 & \Delta_3 & 0 & 0 & 0 \\ 0 & 0 & 0 & 0 & 0 & \Delta_{13} & 0 & 0 \\ 0 & 0 & 0 & 0 & 0 & 0 & \Delta_{23} & 0 \\ 0 & 0 & 0 & 0 & 0 & 0 & 0 & \Delta_\sigma \end{pmatrix}. \quad (5)$$

Here $D_{ij} = d_i d_j / R_{ij}^3$ is the dipole-dipole coupling of the i th and j th atoms at distance R_{ij} , with d_i the i th atom dipole matrix element, and $V_i = \mathcal{E}_\omega d_i$ is the dipole coupling of the i th atom to the external electromagnetic field. The excitation energy detunings of single atoms $A_i = \hbar(\omega_i^a - \omega)$ determine the detunings of pairs of atoms $A_{ij} = A_i + A_j$ and the total detuning $A_\sigma = A_1 + A_2 + A_3$. Their values can be changed by variation of a static electric field E_S (Stark effect), which results in energy shifts $A_i \rightarrow A_i + \Delta_i$ for single atoms, where $\Delta_i = \alpha_i E_S$ depend on atom-specific electric permeability constants α_i , and similar shifts $\Delta_{ij} = \Delta_i + \Delta_j$ and $\Delta_\sigma = \Delta_1 + \Delta_2 + \Delta_3$ for two and three atomic detunings respectively.

Note that by a proper choice of Δ_i and ω one can set two of the three A_i to zero. Moreover, to simplify the presentation we also set to zero the third A_i , which would otherwise remain just a part of \hat{H}_0 . Hence, hereafter all Δ_i denote just the deviations from zero resulting from the variation of the Stark field E_S . The latter together with the amplitude \mathcal{E}_ω serve as time dependent control parameters, C_S and C_ω respectively. The matrices \hat{P}_S and \hat{P}_ω contain therefore only the permeabilities α_i and the dipole moments d_i respectively.

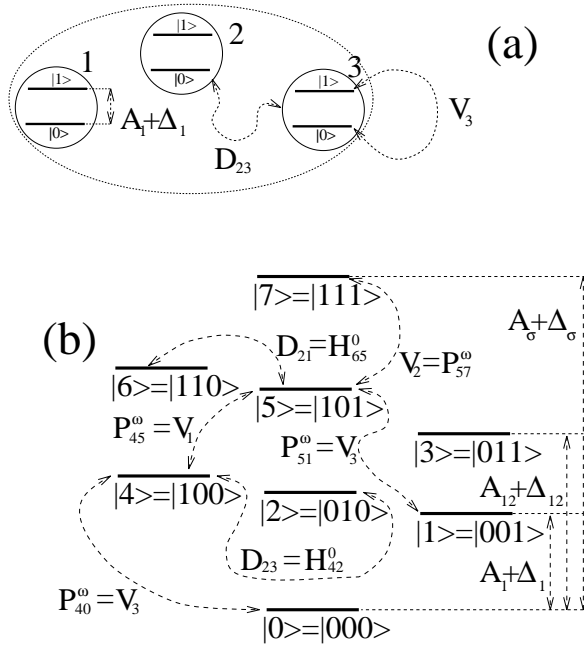


FIG. 1. Realization of a unit cell: A compound system of three two-level atoms interacting with external electromagnetic and static electric fields. (a) The i th atom has ground and excited states $|0\rangle_i$ and $|1\rangle_i$ with excitation energy $A_i + \Delta_i$ that can be modified by the static field; transition amplitude in the electromagnetic field is V_i ; the dipole-dipole coupling of the i th and j th atoms is D_{ij} . (b) The computational basis states and their relation to matrix elements of the principal Hamiltonian \hat{H}_0 and the perturbations \hat{P}_ω and \hat{P}_S of Eqs. (3-5).

B. Cell control

To exert direct universal control over the unit cell we proceed as follows. (i) We fix $N^2 = 64$ consecutive time intervals of equal duration T in which the two perturbations will be applied to the system in an alternating sequence: in the k th interval the perturbation is $\hat{P}_k = \hat{P}_S$ for odd k and $\hat{P}_k = \hat{P}_\omega$ for even k , where $k = 1, 2, \dots, 64$. The strength of \hat{P}_k is a controllable parameter, which we take to have a constant value C_k , and which denotes either \mathcal{E}_ω or E_S , during the k -th time interval, depending on the parity of k [19]. Thus, the system evolution is given by a Hamiltonian which is constant in each interval:

$$\hat{H}(t) = \hat{H}_0 + C_k \hat{P}_k \quad t \in [(k-1)T, kT]. \quad (6)$$

(ii) We find 64 positive C_k values for which the total evolution of the system will be the identity transformation:

$$\hat{U}(t = 64T) \equiv \prod_{k=1}^{64} \exp \left[-\frac{i}{\hbar} (\hat{H}_0 + C_k \hat{P}_k) T \right] = \hat{I}. \quad (7)$$

To this end, we first solve the “8th root” of Eq. (7),

$$\hat{U}(t = 8T) \equiv \prod_{k=1}^8 \exp \left[-\frac{i}{\hbar} (\hat{H}_0 + C_k \hat{P}_k) T \right] = \hat{I}^{1/8}, \quad (8)$$

by minimizing the coefficients of the characteristic polynomial of $\hat{U}(t = 8T)$ [14]. This gives a sequence of positive values, C_1, C_2, \dots, C_8 , for which $\hat{U}(t = 8T)$ has the eigenvalues $e^{2\pi i m/8}$, $m = 1, 2, \dots, 8$, and hence satisfies $[\hat{U}(t = 8T)]^8 = \hat{I}$ nondegenerately. Repeating this sequence 8 times we obtain the required 64 C_k . (iii) Now, by small variations δC_k of the C_k values we can obtain any unitary transformation \hat{U}_ϵ in a small neighborhood of the identity transformation:

$$\hat{U}(t = 64T) \equiv \prod_{k=1}^{64} \exp \left[-\frac{i}{\hbar} (\hat{H}_0 + [C_k + \delta C_k] \hat{P}_k) T \right] = \hat{U}_\epsilon. \quad (9)$$

Indeed, we can present this “small” transformation as

$$\hat{U}_\epsilon = \exp(-i\hat{\mathcal{H}}\epsilon), \quad (10)$$

with dimensionless 8×8 Hermitian Hamiltonian $\hat{\mathcal{H}}$ which is bounded as $\|\hat{\mathcal{H}}\| \leq 1$ and is multiplied by a small parameter $\epsilon > 0$. Now the variations δC_k are determined to first order in ϵ by the linear equations

$$\sum_{k=1}^{64} \frac{\partial \hat{U}(t = 64T)}{\partial C_k} \delta C_k = -i\hat{\mathcal{H}}\epsilon. \quad (11)$$

Moreover, when ϵ is sufficiently small, iterative Newton method refinements of the δC_k yield $\hat{U}(t = 64T) = \hat{U}_\epsilon$

with utmost accuracy [14]. (iv) Finally, to perform an arbitrary unitary transformation we again present it as U_ϵ in Eq. (10), but now the parameter ϵ may take any value in $[0, 2\pi]$ and will not necessarily be small. We effect the \hat{U}_ϵ by dividing it into “small” steps: we apply the transformation $\hat{U}(t = 64T) = \hat{U}_{\epsilon/m}$ repeatedly m times, with m big (ϵ/m small) enough to allow direct control, and obtain

$$\hat{U}(t = 64mT) = (\hat{U}_{\epsilon/m})^m = \hat{U}_\epsilon. \quad (12)$$

We note that, for the problem under consideration, direct control is typically attainable with $m \leq 16$. Moreover, we expect that $m = 1$ will be sufficient with more powerful numerical methods for solving Eq. (9) [15]. Thus, in contrast with earlier control schemes [3,8,9], the desired unitary transformation is effected within a few control cycles, with accuracy that depends in principle only on the physical precision of the controls.

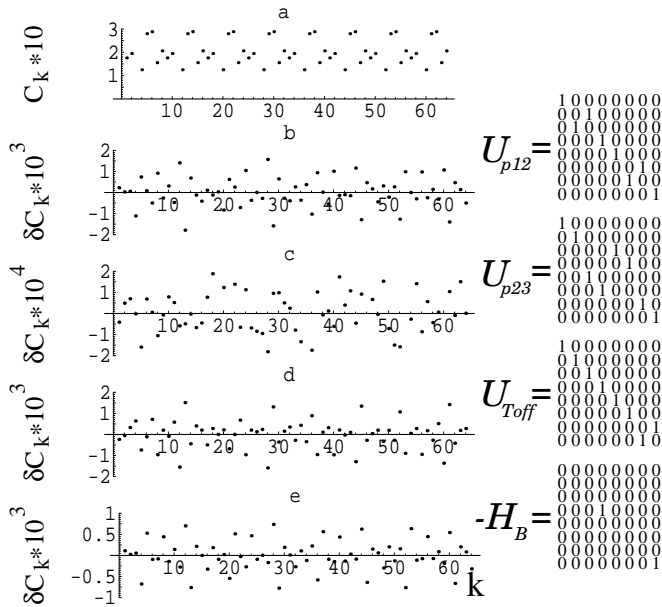


FIG. 2. (a) Control parameters C_k for the identity transformation \hat{I} . Variations δC_k effecting on the cell the transformation $\hat{U}_{\epsilon/8}$, with $\hat{U}_\epsilon \equiv (\hat{U}_{\epsilon/8})^8$ equal to: (b) the permutation \hat{U}_{p12} ; (c) the permutation \hat{U}_{p23} ; (d) the Toffoli-gate transformation \hat{U}_{Toff} . (e) Variations δC_k effecting the conditional phase shift $\hat{B}(\phi) = \exp(-i\phi\hat{\mathcal{H}}_B)$, at $\phi = \pi/32$, employed in the quantum discrete Fourier transform.

In Fig. 2 we show examples of unit cell control, where appropriately chosen parameters C_k and variations δC_k effect unitary transformations on the unit cell: the Toffoli-gate transformation (see Appendix A), two-qubit permutations $\hat{p}_{ij}|a\rangle_i|b\rangle_j = |b\rangle_i|a\rangle_j$ ($a, b = 0, 1$), and the conditional phase shift employed in the quantum discrete Fourier transform (discussed in Sec. V). The transformation is achieved either directly ($m = 1$) or by 8 repeti-

tions ($m = 8$). The operators \hat{H}_0 , \hat{P}_ω and \hat{P}_S are chosen with arbitrary realistic values. We take $D_{12} = 1.1E_u$, $D_{23} = 0.946E_u$, $D_{13} = 0.86E_u$, and $T = 250\hbar/E_u$, where $E_u \sim 10^{-18}$ erg is the typical energy scale. For odd k we switch off the external electromagnetic field, $V_{1;2;3} = 0$, and tune the atomic excitation energies by the Stark field E_S such that $\Delta_{1;2;3} = (0.1; 0.11; 0.312)E_u$. For even k we set $E_S = 0$, that is $\Delta_{1;2;3} = 0$, and take $V_{1;2;3} = (0.3; 0.33; 0.24)E_u$.

IV. COMPLETELY CONTROLLED QUANTUM DEVICES

Once completely controlled unit cells can be constructed, a compound device can be assembled from such elements. To be efficient, the architecture of the device will depend on the specific function it should perform. In Fig. 3 we show two possible arrangements of unit cells for special purpose devices: the first arrangement suites more the purpose of quantum computing, while the second is more useful for simulating lattice quantum field dynamics.

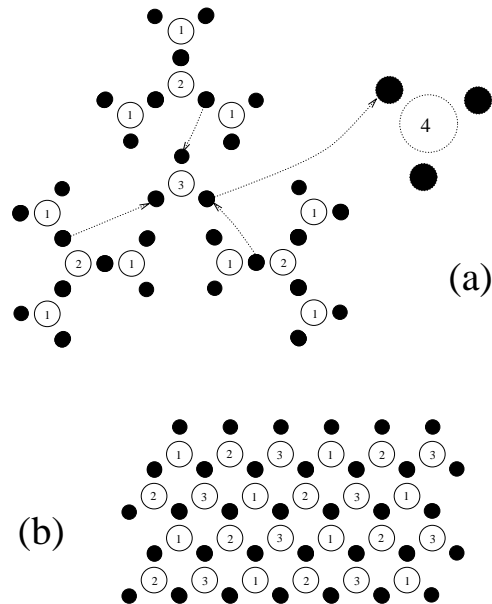


FIG. 3. Two possible arrangements of cells for special purpose devices: (a) tree-like structure for quantum computation; (b) planar lattice for simulating dynamics of quantum fields. The circled numbers denote the rank of joints of the tree (a) or specify the order in which atoms are grouped into triads (b). The arrows show state exchange to parent joints.

The first device (Fig. 3(a)) is organized in a tree-like structure, where the quantum state of one atom in each cell can be exchanged with the state of an atom at the closest parent joint of the tree. The simplest way to make the exchange is to displace the atom to the parent joint, however, the exchange or transport of the state without moving the atom can be more practical. The tree-like ar-

chitecture and the possibility to perform all the unitary transformations, including all the permutations, in each unit cell allow one to put together and make interfering the states of any three two-level atoms of the device after at most $s = 6 \log_3 n$ state exchanges, by moving them toward the root of the tree to a common cell. Placing the new states back (if needed) requires the same number of inverse exchanges. This is a very modest number, $s \sim 40$, even for a rather large device of $n \sim 10^3$ with Hilbert space of $N = 2^n \sim 10^{300}$ dimensions. Hence, all basic operations of quantum computation can be performed on any physical system comprised of non-holonomic triads of two-level subsystems in a tree-like structure, and each operation can be completed within $64 \times 16 \times 12 \times \log_3 n$ control intervals T . Note that the unity transformation should be applied to all other cells to preserve their states during the operation.

The second arrangement of cells (Fig. 3(b)) is intended mainly for emulating the dynamics of quantum fields on lattices. Of course, it can also perform general operations on any triad, but for a higher cost of $s = O(n^{1/2})$. In this arrangement, after each control period of $64T$ the closest neighboring atoms are differently regrouped in triads (cells), with the original grouping repeating itself after three consecutive periods. Therefore, at each moment the change of the cell state depends on the states of the neighboring cells, as it should be in order to emulate the dynamics of the fields. Immediate analogy to the Ising model emerges when we restrict ourselves to small values of ϵ where terms of order ϵ^2 are negligible, and then each $64T$ period plays the role of the time increment $\Delta\tau = \epsilon$. The evolution of such device is determined by three sums of effective cell Hamiltonians, $\hat{H}_{eff}^{(p)} = \sum_q \hat{\mathcal{H}}_{q,p}$, one for each period $p = 1, 2, 3$, where $\hat{\mathcal{H}}_{q,p}$ is the effective Hamiltonian of the q th cell at the p th period.

We can cast the cell Hamiltonians to sums of tensor products of Pauli matrices $\hat{\sigma}_\alpha^i$, where the Greek index $\alpha = x, y, z$ denotes the matrix type and the Latin index i specifies the two-level atom on which it acts. Since the cells are under complete control, the coefficients of this development can be made an arbitrary function of the time τ , and hence the effective Hamiltonian reads

$$\begin{aligned} \hat{H}_{eff}(\tau) = & A_i^\alpha(\tau) \hat{\sigma}_\alpha^i + B_{(i,j)}^{\alpha\beta}(\tau) \hat{\sigma}_\alpha^i \hat{\sigma}_\beta^j \\ & + C_{(i,j,k)}^{\alpha\beta\gamma}(\tau) \hat{\sigma}_\alpha^i \hat{\sigma}_\beta^j \hat{\sigma}_\gamma^k, \end{aligned} \quad (13)$$

with implicit summation over repeated indices, where (i, j) and (i, j, k) indicate pairs and triads of distinct atoms that are periodically grouped in a common cell. This Hamiltonian results in the evolution equation for the Heisenberg operators $\hat{\sigma}_\alpha^i(\tau)$,

$$\begin{aligned} \hbar \frac{d\hat{\sigma}_\alpha^i(\tau)}{d\tau} = & \mathcal{A}_{\alpha,j}^{i,\beta}(\tau) \hat{\sigma}_\beta^j(\tau) + \mathcal{B}_{\alpha,(j,k)}^{i,\beta\gamma}(\tau) \hat{\sigma}_\beta^j(\tau) \hat{\sigma}_\gamma^k(\tau) \\ & + \mathcal{C}_{\alpha,(j,k,l)}^{i,\beta\gamma\delta}(\tau) \hat{\sigma}_\beta^j(\tau) \hat{\sigma}_\gamma^k(\tau) \hat{\sigma}_\delta^l(\tau), \end{aligned} \quad (14)$$

where the coefficients $\mathcal{A}, \mathcal{B}, \mathcal{C}$ are determined by A, B, C and the commutation relations of the Pauli matrices. By

a proper choice of the coefficients A, B, C through the appropriate control sequences, one can simulate different linear and non-linear lattice models of quantum fields with time dependent parameters.

V. TOY DEVICE

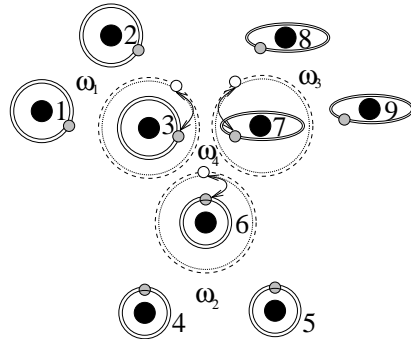


FIG. 4. A toy device, composed of 9 Rydberg atoms, that can perform quantum computations on 9 qubits. Each atom is a two-level system shown schematically by double orbits. Atoms of different triads are excited to distinct pairs of Rydberg states. Each triad p is controlled by an external field of distinct frequency ω_p . One atom in each triad can be excited to a pair of higher Rydberg states, thus forming a higher-level triad: (3,6,7). These excitations (depicted by arrows) correspond to state transportations.

We now describe a toy device that can perform quantum computations on 9 qubits. An ensemble of 9 different Rydberg atoms is placed in a magneto-optical trap at low temperature, as illustrated in Fig. 4. By different atoms we mean atoms of different elements or identical atoms that are excited to distinct pairs of Rydberg states. The best candidates for such a device are the long-living states corresponding to large angular momentum. By placing all the atoms in a static electric field one lifts the degeneracy of the magnetic quantum number and performs tuning if needed. All the atoms experience the dipole-dipole interaction $\hat{D}_{ij} = \hat{d}_i \hat{d}_j \langle R_{ij}^{-3} \rangle$, where the cube of the inverse distance between atoms is averaged over their translational quantum states. Note, however, that only for almost resonant atoms this interaction is important. By a proper choice of the atomic states and the static field E_S , we obtain three triads, $p = 1, 2, 3$, each comprised of three almost resonant two-level atoms with transition frequencies centered around a distinct frequency ω_p . For each triad p , the interactions \hat{D}_{ij} give the principal Hamiltonian, while a microwave field E_{ω_p} at the frequency ω_p serves as a control perturbation. Transportation of the state of one atom in each triad to the parent joint can be performed by dipole or Raman π transitions from the initial pair of Rydberg levels to a higher pair. With these higher pairs assumed

nearly resonant with a frequency ω_4 , atoms 3, 6 and 7 form a higher-level triad—the parent joint of the first three triads—which is controlled by a fourth microwave field E_{ω_4} of frequency ω_4 .

As an example of implementing quantum computation in the toy device, using our non-holonomic control scheme, we show how to perform the discrete Fourier transform modulo $N = 2^9 = 512$ [20]. This is the unitary transformation on 9 qubits that is given by

$$\hat{F}_N|x\rangle = \frac{1}{\sqrt{N}} \sum_{y=0}^{N-1} \exp(2\pi ixy/N)|y\rangle, \quad (15)$$

where $|x\rangle$ and $|y\rangle$ are states of the system computational basis. The computational basis states are defined as

$$|x\rangle \equiv |x_8\rangle_9 \dots |x_1\rangle_2 |x_0\rangle_1, \quad (16)$$

with $x \equiv \sum_{r=0}^8 x_r 2^r = 0, 1, \dots, N-1$ ($x_r = 0, 1$), where $| \cdot \rangle_i$ denotes the state of the i th atom—the i th qubit. The algorithm we employ to perform the Fourier transform is based on constructing the exponent in Eq. (15) as

$$\exp(2\pi ixy/2^9) = \prod_{r=0}^8 \prod_{s=0}^r \exp(i\pi x'_r y_s / 2^{r-s}), \quad (17)$$

where $x'_r \equiv x_{8-r}$. We begin by reversing the order in which the bits of the input x are stored in our 9-qubit register, that is, we effect the unitary transformation

$$|x_8\rangle_9 \dots |x_1\rangle_2 |x_0\rangle_1 \rightarrow |x_0\rangle_9 \dots |x_7\rangle_2 |x_8\rangle_1 \quad (18)$$

by applying a sequence of state exchanges [21]. Then we complete the transform in 9 steps: (i) We “split” the first qubit (the state of atom 1) by applying the unitary transformation

$$\hat{A} \equiv \frac{1}{\sqrt{2}} \begin{pmatrix} 1 & 1 \\ 1 & -1 \end{pmatrix} = \exp\left[\frac{-i\pi}{\sqrt{8}} \begin{pmatrix} 1-\sqrt{2} & 1 \\ 1 & -1-\sqrt{2} \end{pmatrix}\right], \quad (19)$$

which maps $|0\rangle \rightarrow \frac{1}{\sqrt{2}}(|0\rangle + |1\rangle)$ and $|1\rangle \rightarrow \frac{1}{\sqrt{2}}(|0\rangle - |1\rangle)$. Note that this would already complete the Fourier transform if we had only one qubit. (ii) Next, we apply to the first and second qubits the conditional phase shift $|a\rangle_2|b\rangle_1 \rightarrow e^{i\pi ab/2}|a\rangle_2|b\rangle_1$ ($a, b = 0, 1$), given explicitly by

$$\hat{B}_{21} \equiv \begin{pmatrix} 1 & 0 & 0 & 0 \\ 0 & 1 & 0 & 0 \\ 0 & 0 & 1 & 0 \\ 0 & 0 & 0 & e^{i\pi/2} \end{pmatrix} = \hat{B}(\pi/2), \quad (20)$$

where $\hat{B}(\phi)$ is the unitary transformation

$$\hat{B}(\phi) = \exp[-i\phi \begin{pmatrix} 0 & 0 & 0 & 0 \\ 0 & 0 & 0 & 0 \\ 0 & 0 & 0 & 0 \\ 0 & 0 & 0 & -1 \end{pmatrix}]. \quad (21)$$

Then we “split” the second qubit by applying to it the transformation \hat{A} . This accounts for the contribution of the second most significant bit of the input x . (iii) Similarly, in steps $i = 3, 4, \dots, 9$ we apply the conditional phase shift $|a\rangle_i|b\rangle_j \rightarrow e^{i\pi ab/2^{i-j}}|a\rangle_i|b\rangle_j$ ($a, b = 0, 1$), that is,

$$\hat{B}_{ij} \equiv \begin{pmatrix} 1 & 0 & 0 & 0 \\ 0 & 1 & 0 & 0 \\ 0 & 0 & 1 & 0 \\ 0 & 0 & 0 & e^{i\pi/2^{i-j}} \end{pmatrix} = \hat{B}(\pi/2^{i-j}), \quad (22)$$

to each pair of qubits (i, j) , $j = 1, 2, \dots, i-1$, and then apply the transformation $\hat{A}_i \equiv \hat{A}$ to the i th qubit. Note that after the i th step the first i qubits store the Fourier transform of the i most significant bits of x . Hence, after the 9th step the Fourier transform is completed:

$$\hat{F}_{2^9} = (\hat{A}_9 \hat{B}_{98} \dots \hat{B}_{91}) \dots (\hat{A}_3 \hat{B}_{32} \hat{B}_{31}) (\hat{A}_2 \hat{B}_{21}) (\hat{A}_1). \quad (23)$$

Performing these operations implies also application of state exchanges whenever one needs to transfer the states of atoms i and j to a common unit cell for processing. A list of control commands (δC_k sequences) corresponding to Eqs. (18) and (23) can be written straightforwardly.

VI. CONCLUSION

We have shown that quantum devices with exponentially large Hilbert space dimension can be efficiently controlled, provided they are assembled from completely controllable unit cells in an architecture that is optimized for the specific function they should perform. The unit cell can be constructed from simple quantum objects of arbitrary physical nature: two-level atoms, nuclear spins, rotating molecules, quantum dots, etc. This allows to optimize critical properties such as coherence time and control precision for practical realizations. The only requirement is that the unit cell could be put under non-holonomic control, i.e., that it could be sufficiently perturbed to have unconstrained dynamics. This ensures that the cell can be fully controlled and made perform any desired operation.

As a concrete example, we have considered a quantum system of 2^n levels, composed of n two-level atoms that are coupled by dipole-dipole interactions. The atoms are grouped into unit cells, each consisting of three nearly resonant atoms. Each cell is controlled with two time-dependent perturbations: a static electric field and an electromagnetic field nearly resonant with the atoms. We have shown that any unitary transformation in the $2^3 = 8$ dimensional Hilbert space of the cell can be effected within a few control cycles, each comprising 64 applications of the perturbations with values fixed according to a non-holonomic control scheme. In particular, the Toffoli-gate transformation on the cell regarded as a 3-qubit register and any permutation of the three

qubits can be performed. We have given two examples of function-specific devices that can be assembled from such cells: (i) By arranging the cells in a ternary tree-like structure, we obtain a device that can perform efficient quantum computations on n qubits: any unitary transformation on any three qubits can be effected within order of $\log_3 n$ control cycles. We have described a toy device that can perform computations on 9 qubits, including, for example, the discrete Fourier transform. (ii) When the atoms are arranged in a planar lattice structure, where at each control cycle the closest neighboring atoms are differently grouped in triads, we can simulate various linear and non-linear lattice models of quantum fields with time dependent parameters.

ACKNOWLEDGMENTS

The authors are grateful to M. Gromov for discussions and stimulating remarks. G.H. acknowledges support from the Foundation for Fundamental Research on Matter (FOM), which is financially supported by the Netherlands Organization for Scientific Research (NWO).

APPENDIX A:

The Toffoli-gate transformation is the unitary transformation on three qubits,

$$\hat{U}_{Toff}|x_2\rangle|x_1\rangle|x_0\rangle = |x_2\rangle|x_1\rangle|x_0 \text{ XOR } (x_1 \text{ AND } x_2)\rangle, \quad (\text{A1})$$

which corresponds to the three-bit classical logic gate,

$$\begin{aligned} x_2 &\rightarrow x'_2 = x_2 \\ x_1 &\rightarrow x'_1 = x_1 \\ x_0 &\rightarrow x'_0 = x_0 \text{ XOR } (x_1 \text{ AND } x_2), \end{aligned} \quad (\text{A2})$$

introduced by Toffoli as a universal gate for classical reversible computation [22]. It acts as a permutation of the computational basis states, $|x\rangle \equiv |x_2\rangle|x_1\rangle|x_0\rangle$, $x \equiv \sum_{r=0}^2 x_r 2^r = 0, 1, \dots, 7$, given by the unitary matrix

$$\hat{U}_{Toff} = \begin{pmatrix} 1 & 0 & 0 & 0 & 0 & 0 & 0 & 0 \\ 0 & 1 & 0 & 0 & 0 & 0 & 0 & 0 \\ 0 & 0 & 1 & 0 & 0 & 0 & 0 & 0 \\ 0 & 0 & 0 & 1 & 0 & 0 & 0 & 0 \\ 0 & 0 & 0 & 0 & 1 & 0 & 0 & 0 \\ 0 & 0 & 0 & 0 & 0 & 1 & 0 & 0 \\ 0 & 0 & 0 & 0 & 0 & 0 & 0 & 1 \\ 0 & 0 & 0 & 0 & 0 & 0 & 1 & 0 \end{pmatrix}. \quad (\text{A3})$$

This matrix can be presented as

$$\hat{U}_{Toff} = \exp(-i\pi\hat{\mathcal{H}}_{Toff}), \quad (\text{A4})$$

with the (idempotent) Hermitian matrix

$$\hat{\mathcal{H}}_{Toff} = \frac{1}{2} \begin{pmatrix} 0 & 0 & 0 & 0 & 0 & 0 & 0 & 0 \\ 0 & 0 & 0 & 0 & 0 & 0 & 0 & 0 \\ 0 & 0 & 0 & 0 & 0 & 0 & 0 & 0 \\ 0 & 0 & 0 & 0 & 0 & 0 & 0 & 0 \\ 0 & 0 & 0 & 0 & 0 & 0 & 0 & 0 \\ 0 & 0 & 0 & 0 & 0 & 0 & 1 & -1 \\ 0 & 0 & 0 & 0 & 0 & 0 & -1 & 1 \end{pmatrix}. \quad (\text{A5})$$

In our control scheme the Toffoli-gate transformation can be effected on the unit cell by repeating 8 times the transformation $\hat{U}_{\epsilon/8} \equiv \exp(-i\pi\hat{\mathcal{H}}_{Toff}/8)$ ($\epsilon = \pi$), which is directly attainable: $\hat{U}(t = 64T) = \hat{U}_{\epsilon/8}$ (see Fig. 2(d)).

-
- [1] R. P. Feynman, *Int. J. Theor. Phys.* **21**, 467 (1982).
 - [2] G. M. Huang, T. J. Tarn, and J. W. Clark, *J. Math Phys.* **24**, 2608 (1983).
 - [3] D. Deutsch, *Proc. R. Soc. London A* **400**, 96 (1985); *ibid.* **425**, 73 (1989).
 - [4] D. J. Tannor and S. A. Rice, *J. Chem. Phys.* **83**, 5013 (1985); D. J. Tannor, R. Kosloff, and S. A. Rice, *J. Chem. Phys.* **85**, 5805 (1986).
 - [5] M. Shapiro and P. Brumer, *J. Chem. Phys.* **84**, 4103 (1986); P. Brumer and M. Shapiro, *Chem. Phys. Lett.* **126**, 54 (1986).
 - [6] A. P. Peirce, M. A. Dahleh, and H. Rabitz, *Phys. Rev. A* **37**, 4950 (1988); R. S. Judson and H. Rabitz, *Phys. Rev. Lett.* **68**, 1500 (1992); V. Ramakrishna, M. V. Salapaka, M. Dahleh, H. Rabitz, and A. Peirce, *Phys. Rev. A* **51**, 960 (1995); V. Ramakrishna and H. Rabitz, *Phys. Rev. A* **54**, 1715 (1996).
 - [7] K. Vogel, V. M. Akulin, and W. P. Schleich, *Phys. Rev. Lett.* **71**, 1816 (1993).
 - [8] S. Lloyd, *Science* **261**, 1569 (1993); S. Lloyd, *Phys. Rev. Lett.* **75**, 346 (1995); S. Lloyd, *Science* **273**, 1073 (1996).
 - [9] D. P. DiVincenzo, *Phys. Rev. A* **51**, 1015 (1995).
 - [10] J. I. Cirac and P. Zoller, *Phys. Rev. Lett.* **74**, 4091 (1995).
 - [11] G. Harel, G. Kurizki, J.K. McIver, and E. Coutsias, *Phys. Rev. A* **53**, 4534 (1996).
 - [12] C. K. Law and J. H. Eberly, *Phys. Rev. Lett.* **76**, 1055 (1996).
 - [13] For reviews on quantum computation see: A. Ekert and R. Jozsa, *Rev. Mod. Phys.* **68**, 733 (1996); J. Preskill, *Proc. R. Soc. London A* **454**, 469 (1998) (LANL e-print quant-ph/9705032).
 - [14] G. Harel and V. M. Akulin, *Phys. Rev. Lett.* **82**, 1 (1999).
 - [15] V. Gershkovich *et al.*, to be published (IHES preprint IHES/P/00/01).
 - [16] We do not consider here the important issue of decoherence and error correction, since the correction procedure can be treated as a particular case of operating the quantum device.

- [17] One can prove that a system comprised of two non-holonomic parts, with an interaction that cannot be represented as a single tensor product of operators related to each part, is in itself non-holonomic; see Ref. [15].
- [18] More Precisely, $i\hat{H}_0$, $i\hat{P}_\omega$, $i\hat{P}_S$, and their commutators of all orders must span the 64-dimensional real linear space of 8×8 anti-Hermitian matrices.
- [19] In the notation of Eq. (1), for $t \in [(k-1)T, kT]$ we have $\hat{H}(t) = \hat{H}_0 + C_S(t)\hat{P}_S + C_\omega(t)\hat{P}_\omega$, with $C_\omega(t) = 0$ and $C_S(t) = C_k$ for odd k , and $C_S(t) = 0$ and $C_\omega(t) = C_k$ for even k .
- [20] The quantum discrete Fourier transform is reviewed in Ekert and Jozsa, Ref. [13]. An early proposal for its physical implementation was given by Cirac and Zoller, Ref. [10].
- [21] This reversal can be avoided if we agree to read the result in the bit-reversed order; see Ekert and Jozsa, Ref. [13].
- [22] T. Toffoli, *Math. Systems Theory* **14**, 13 (1981); see also A. Barenco, C. H. Bennett, R. Cleve, D. P. DiVincenzo, N. Margolus, P. Shor, T. Sleator, J. A. Smolin, and H. Weinfurter, *Phys. Rev. A* **52**, 3457 (1995).